Bulk and Interface effects on voltage linearity of ZrO_2-SiO_2 multilayered metal-insulator-metal capacitors for analog mixed-signal applications

S. D. Park,[1] C. Park,[1,a)] D. C. Gilmer,[1] H. K. Park,[1] C. Y. Kang,[1] K. Y. Lim,[1] C. Burham,[1] J. Barnett,[1] P. D. Kirsch,[1] H. H. Tseng,[1] R. Jammy,[1] and G. Y. Yeom[2]

[1]*SEMATECH, 2706 Montopolis Dr., Austin, Texas 78741, USA*

[2]*Department of Materials Science and Engineering, Sungkyunkwan University, Suwon, Kyunggi-do 440-746, Republic of Korea*

(Received 1 April 2009; accepted 28 June 2009; published online 16 July 2009)

Quadratic voltage coefficient of capacitance (VCC) for ZrO_2-SiO_2 multilayered dielectric metal-insulator-metal capacitors depends strongly on the stacking sequence of the layered dielectrics. The quadratic VCC of an optimized $SiO_2/ZrO_2/SiO_2$ stack and $ZrO_2/SiO_2/ZrO_2$ stack were +42 and −1094 ppm/V^2, respectively, despite the same total SiO_2 and ZrO_2 dielectric thickness in the stack. The observed difference in quadratic VCC depending on dielectric stacking sequence is explained by taking into account both the interface and bulk dielectric responses to the applied voltage. © *2009 American Institute of Physics*. [DOI: 10.1063/1.3182856]

The metal-insulator-metal (MIM) capacitor is one of the main components of analog/mixed-signal integrated circuits and radio frequency devices.[1,2] The key figures of merit used to characterize MIM capacitors are capacitance density ($C_{density}$) and capacitance voltage nonlinearity.[3] Higher $C_{density}$ is required for capacitor area scaling, which results in increased circuit density and reduced system cost. Reduced capacitance nonlinearity is a benchmark to improve the accuracy of the passive components, since shifts in capacitance can lead to distortions in analog signals or can be upconverted to higher frequencies in mixers and nonlinear circuit applications.[4] The voltage nonlinearity of capacitance is characterized by the quadratic equation in voltage

$$\frac{\Delta C}{C_0} = \frac{C(V) - C_0}{C_0} = \alpha V^2 + \beta V,$$

where C_0 is the capacitance at zero-bias and α and β are the quadratic and linear coefficients of the capacitor, respectively.[4] The quadratic voltage nonlinearity is inversely proportional to the dielectric thickness $(1/t_{ox}^2)$;[5] therefore, α and $C_{density}$ are in a trade-off relationship, making the simultaneous achievement of large $C_{density}$ and linearity difficult. Shown in Fig. 1 is published data for voltage coefficient of capacitance (VCC) versus $C_{density}$ plotted along with results of the present work. Many high-k dielectrics, such as HfO_2,[1] Ta_2O_5,[6,7] and Al_2O_3,[7] have been investigated as an insulator in MIM capacitors, however, there is no known single-layer high-k dielectric MIM capacitor that meets the International Technology Roadmap for Semiconductors (ITRS) guidelines for 2012 ($C_{density} > 5$ fF/μm^2, $\alpha < 100$ ppm/V^2, and leakage current $< 10^{-8}$ A/cm^2).[3] Numerous MIM capacitors with various bilayer, sandwiched, and laminated dielectrics have also been investigated.[6–10] Among these multilayered dielectric stack MIM capacitors, only the HfO_2/SiO_2 bilayer dielectric seems to meet the ITRS guidelines (shaded area in Fig. 1).[10]

Despite numerous efforts to improve the voltage linearity of MIM capacitors, the basic mechanism controlling the α of the MIM capacitor is not yet well understood. Several models have been proposed to explain its voltage linearity, such as the occurrence of free carrier space charge relaxation,[11] nonlinearities of the metal-oxygen bond polarizability,[12] or electrode coupling and "hopping" conduction between vacancy sites.[13] These models explain voltage linearity either by a dielectric bulk effect or dielectric/electrode interface effect.

In our study, voltage linearity of MIM capacitors with asymmetric bilayered and symmetric trilayered ZrO_2-SiO_2 dielectric stacks deposited in various sequences were investigated to study the mechanism of capacitance variation, taking into account both the dielectric bulk and dielectric/electrode interface characteristics. By combining a high dielectric constant (~39) ZrO_2 having positive α with high band gap SiO_2 having negative α, along with interface engineering, we were able to fabricate MIM capacitors with high $C_{density}$ and low α as well as low leakage current.

MIM capacitors were fabricated by using TiN as both top and bottom electrodes. Dielectric film thickness was measured by ellipsometer. Capacitors with different areas were defined by photolithography and plasma etching. The typical capacitor area was 0.01 mm^2 (100×100 μm^2).

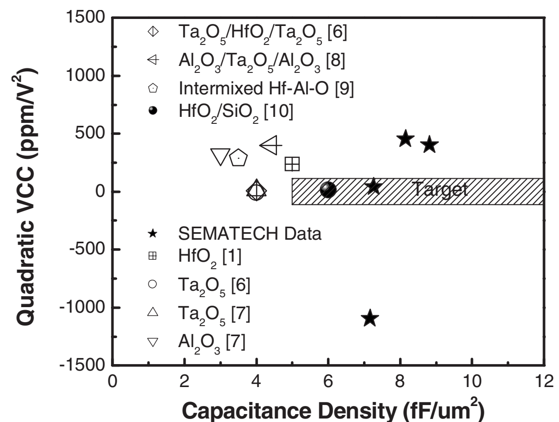

FIG. 1. Comparisons of high-k MIM capacitors electrical results from this work along with reports in the literature and the ITRS technology requirements for analog/mixed-signal capacitors.

a)Author to whom correspondence should be addressed. Electronic mail: chanro.park@sematech.org.

 © 2009 American Institute of Physics

Downloaded 17 Jul 2009 to 192.73.53.5. Redistribution subject to AIP license or copyright; see http://apl.aip.org/apl/copyright.jsp

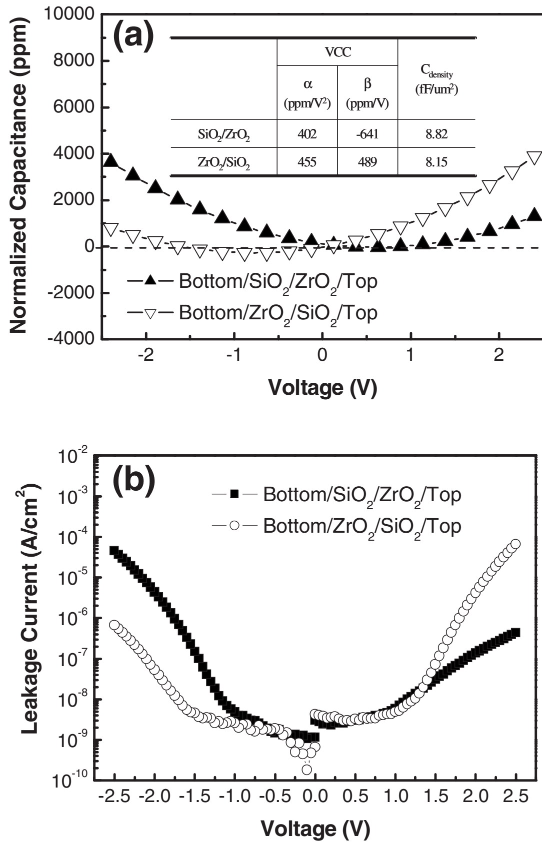

FIG. 2. (a) Normalized capacitance characteristics for a MIM capacitor with ZrO_2/SiO_2 bilayer stack and (b) *I-V* characteristics of such a structure. The inset shows VCC α and β and capacitance density ($C_{density}$) as a function of the dielectric stack sequence.

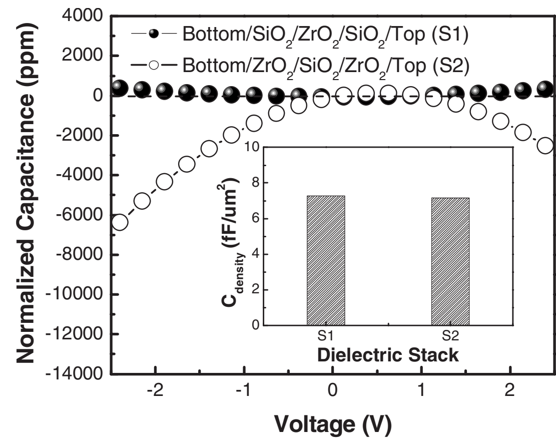

FIG. 3. Normalized capacitance of MIM capacitors with $SiO_2/ZrO_2/SiO_2$ and $ZrO_2/SiO_2/ZrO_2$ stacks. Both stacks, denoted as S1 and S2, respectively, have similar capacitance density, as the inset shows, but significantly different quadratic VCC values depending on the dielectric deposition sequence.

Capacitance-voltage (*C-V*) measurements were performed on a precision *LCR* meter (Hewlett-Packard, 4284A) at 100 kHz with a (25 mV) ac sweeping signal. Current-voltage (*I-V*) characteristics were measured using a semiconductor parameter analyzer (Hewlett-Packard, 4156B). For all *C-V* and *I-V* measurements, the potentials were referred to the bottom electrode, creating an electron injection from the bottom electron with positive bias. Capacitance has been normalized to the capacitance measured at 0 V dc bias across the capacitor.

Figure 2 shows (a) the normalized capacitance characteristics for a MIM capacitor with ZrO_2/SiO_2 bilayer stack and (b) the *I-V* characteristics of such a structure. These MIM capacitors have the same SiO_2 and ZrO_2 thickness, but in reverse order. As shown in Figs. 2(a) and 2(b), the ZiO_2/SiO_2 bilayer stack MIM capacitor shows asymmetric *C-V* and *I-V* curves depending on the order of the dielectric stack, while both stacks show similar α values. These asymmetric *C-V* and *I-V* curves of the MIM capacitor with the ZrO_2/SiO_2 bilayered stack can be explained by the injected electron density. The injected electron density depends on the barrier height for electron injection between the dielectric and electrode and the defect density of the dielectric.[14] Injected electron density must be lower when electrons are injected into a high band gap SiO_2 rather than lower band gap ZrO_2, since SiO_2 has a greater barrier height and lower defect density than ZrO_2. The asymmetric *C-V* and *I-V* curves, thus, can be ascribed to the asymmetric band diagram of the metal-ZrO_2/SiO_2-metal structure. This result implies that dielectric and electrode interfaces may play an important role to achieve low α and high $C_{density}$ in a MIM capacitor.

Figure 3 shows the normalized capacitance of MIM capacitors with symmetric sandwiched dielectric stacks, but with different stacking order to see the effect of dielectric and electrode interface. The $C_{density}$ for the two different dielectric stacks is nearly the same, as shown in Fig. 3 (inset). The $SiO_2/ZrO_2/SiO_2$ and $ZrO_2/SiO_2/ZrO_2$ structures are denoted by S1 and S2, respectively. The total thicknesses of the ZrO_2 film and SiO_2 film in the symmetric sandwiched dielectric stacks are the same, as confirmed by high resolution transmission electron microscopy images (not shown). The $C_{density}$ of both S1 and S2 are close to 7.2 $fF/\mu m^2$, with an equivalent oxide thickness (EOT) of around 4.8 nm. In contrast, S1 and S2 have very different α values despite their similar EOTs. The extracted α of S1 and S2 are +42 and -1094 ppm/V^2, respectively. If α is solely dictated by bulk dielectric properties,[11,12] there should not be a significant difference in the α of S1 and S2, which have the same total ZrO_2 and SiO_2 thicknesses, but with different stacking sequence. The SiO_2 layer is in contact with the TiN top and bottom electrode in S1, while the ZrO_2 layer is in contact with the TiN electrodes in S2. Alternatively, if α is determined solely by the dielectric/electrode interface effect, such as electrode polarization effect,[13] it is difficult to explain the negative α of S2. Our experimental data suggests that both dielectric bulk and dielectric/electrode interfaces are contributing to the α of the sandwiched structure. When a thin dielectric layer is in contact with electrodes, an electrode polarization exponentially increases the capacitance with applied voltage[13] (dielectric/electrode interface effect layer). When SiO_2 is in contact with the electrode as in S1, the negative α of SiO_2 is negated by the dielectric/electrode interface effect. But when SiO_2 is in the middle of a multilayer dielectric, the negative α characteristic of SiO_2 is maintained. Consequently, although S1 and S2 have the same SiO_2 thickness, the impact of SiO_2 in S2 is greater than in S1 and the α of S2 remains negative.

The impact of the dielectric/electrode interface effect on VCC characteristics for ZrO_2-SiO_2 multilayered MIM capacitors can be examined by using MIM capacitors with a single layer of SiO_2 having different thicknesses. Assuming that the dielectric/electrode interfacial layer is thinner than

Downloaded 17 Jul 2009 to 192.73.53.5. Redistribution subject to AIP license or copyright; see http://apl.aip.org/apl/copyright.jsp

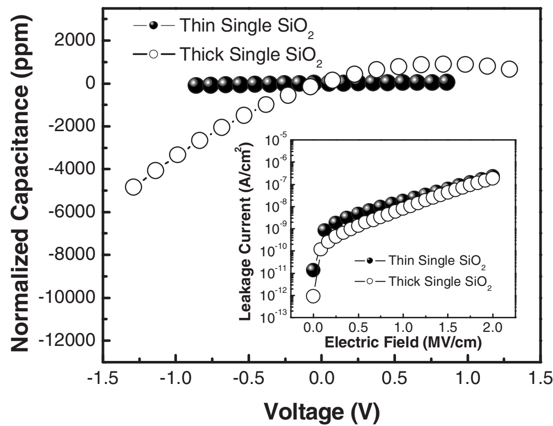

FIG. 4. Normalized capacitance of MIM capacitors with a single-layer SiO_2 dielectric as a function of SiO_2 thickness. The inset shows the leakage current of the MIM capacitor as a function of applied electric field. The capacitances of the thin SiO_2 and thick SiO_2 MIM capacitors are measured from -0.8 to 0.8 V, and from -1.2 to 1.2 V, respectively.

the SiO_2 dielectric thickness, the interface contribution to VCC will be greater as SiO_2 gets thinner. Figure 4 shows the normalized capacitance characteristics for single-layer SiO_2 MIM capacitors and the inset shows the corresponding leakage current as a function of applied electric field. To apply the same electric field to the MIM capacitors, the capacitance and leakage currents are measured with a voltage sweep from -0.8 to 0.8 V, and from -1.2 to 1.2 V, for the thin SiO_2 and thick SiO_2 MIM capacitors, respectively. The leakage currents of both capacitors are close to 2.0×10^{-7} A/cm^2 at an applied electric field of 2 MV/cm. However, the α of thin SiO_2 and thick SiO_2 are -46.5 and -1266.6 ppm/V^2, respectively. This contradicts the thickness dependency of α, which predicts α being inversely proportional to the square of dielectric thickness, $\alpha\sim 1/t_{ox}{}^2$.[5] Since the thickness dependency of α takes into account only the bulk effect of the dielectric, the model fails to predict α of very thin dielectric layers in MIM capacitors where the interface effect is no longer negligible.

The voltage linearity of the high-k MIM capacitors with ZrO_2-SiO_2 layered dielectrics was investigated as a function of stacking sequence. VCC of MIM capacitor was more positive when SiO_2 was in contact with electrodes than that of ZrO_2 being in contact with electrodes with same total SiO_2 and ZrO_2 thicknesses. This supports the concept that both electrode-dielectric interface and bulk dielectric effect play an important role in the voltage linearity of MIM capacitors. Effect of interface on VCC was confirmed with single-layer SiO_2 MIM capacitors, where lower absolute VCC was obtained in thinner SiO_2 in contrast to a model which only took into account bulk contribution to VCC. In addition, it has been shown that a MIM capacitor engineered with a symmetric layered dielectric stack of $SiO_2-ZrO_2-SiO_2$ can meet the ITRS guidelines for 2012.

Part of this work done by SKKU was supported by the National Program for Tera-level Nanodevices of the Korea Ministry of Science and Technology as a 21st Century Frontier Program.

[1] X. F. Yu, C. X. Zhu, H. Hu, A. Chin, M. F. Li, B. J. Cho, D.—L. Kwong, P. D. Foo, and M. B. Yu, IEEE Electron Device Lett. **24**, 63 (2003).
[2] K. Takeda, T. Ishikawa, T. Mine, T. Imai, and T. Fujiwara, Jpn. J. Appl. Phys., Part 1 **46**, 2973 (2007).
[3] The International Technology Roadmap for Semiconductors: Semicond. Assoc. Ind., 2007.
[4] C. H. Ng, C. S. Ho, S. F. S. Chu, and S. C. Sun, IEEE Trans. Electron Devices **52**, 1399 (2005).
[5] T. Iida, M. Nakahara, S. Gotoh, and H. Akida, Proceedings of the IEEE Custom Integration Circuits Conference, 1990 (unpublished), p. 18.5.1.
[6] Y. K. Jeong, S. J. Won, D. J. Kwon, M. W. Song, W. H. Kim, O. H. Park, J. H. Jeong, H. S. Oh, H. K. Kang, and K. P. Suh, VLSI Tech. Dig. Tech. **2004**, 222.
[7] Y. L. Tu, H. L. Lin, L. L. Chao, D. Wu, C. S. Tsai, C. Wang, C. F. Huang, C. H. Lin, and J. Sun, VLSI Tech. Dig. Tech. **2003**, 79.
[8] T. Ishikawa, D. Kodama, Y. Matsui, M. Hiratani, T. Furusawa, and D. Hisamoto, Tech. Dig. - Int Electron Devices Meet. **2002**, 940.
[9] H. Hang, S. J. Ding, H. F. Lim, C. X. Zhu, M. F. Li, S. J. Kim, X. F. Yu, J. H. Chen, Y. F. Yong, B. J. Cho, D. S. H. Chan, S. C. Rustagi, M. B. Yu, C. H. Tung, A. Y. Du, D. My, P. D. Foo, A. Chin, and D. L. Kwong, Tech. Dig. - Int Electron Devices Meet. **2003**, 15.6.1.
[10] S. J. Kim, B. J. Cho, M. F. Li, S. J. Ding, C. Zhu, M. B. Yu, B. Narayanan, A. Chin, and D. L. Kwong, IEEE Electron Device Lett. **25**, 538 (2004).
[11] S. Blonkowski, M. Regache, and A. Halimaoui, J. Appl. Phys. **90**, 1501 (2001).
[12] S. Bécu, S. Crémer, and J. L. Autran, Appl. Phys. Lett. **88**, 052902 (2006).
[13] P. Gonon and C. Vallée, Appl. Phys. Lett. **90**, 142906 (2007).
[14] S. M. Sze, *Physics of Semiconductor Devices* (Wiley, New York, 1998).

Downloaded 17 Jul 2009 to 192.73.53.5. Redistribution subject to AIP license or copyright; see http://apl.aip.org/apl/copyright.jsp